CHEMISTRY
AN ASIAN JOURNAL
www.chemasianj.org

Accepted Article

Title: Self-assembly of Spherical Organic Molecules to form Hollow Vesicular Structure in Water for Encapsulation of an Anti-cancer Drug and Its Release

Authors: Parthasarathi Dastidar, Koushik Sarkar, and Sabir Ahmed

To be cited as: *Chem. Asian J.* 10.1002/asia.201900211

Link to VoR: http://dx.doi.org/10.1002/asia.201900211

A Journal of

ACES
Asian Chemical Editorial Society

A sister journal of **Angewandte Chemie** and **Chemistry – A European Journal**

WILEY-VCH

10.1002/asia.201900211

WILEY-VCH

Self-assembly of Spherical Organic Molecules to form Hollow Vesicular Structure in Water for Encapsulation of an Anti-cancer Drug and Its Release

Koushik Sarkar, Sabir Ahmed and Parthasarathi Dastidar*[a]

Abstract: Developing hierarchical supramolecular structures is important for better understanding of various biological functions and possibly generating new materials for biomedical applications. In here, we report the first examples of functional vesicles derived from cationic spherical organic molecules (**C_1-C_3**) which were readily synthesized by reacting a C_3-symmetric tris-benzimmidazole derivative (possessing a 1,3,5-ethyl substituted aromatic core) with 1,3,5-substituted tris-bromomethyl benzene derivatives. Vesicle formation by **C_1-C_3** was probed by high resolution microscopy (TEM and AFM) dynamic light scattering (DLS) and fluorescence microscopic images of calcein loaded vesicles. One of the vesicles [**Vesicle(C_3)**] displayed the ability to load an anti-cancer drug doxorubicin (**DOX**). The drug was subsequently released from **DOX@Vesicle(C_3)** in a stimuli responsive manner in presence of a well-known vesicle destroyer **Triton X–100** as revealed by *in vitro* cell migration assay carried out on a highly aggressive human breast cancer cell line (**MDA-MB-231**).

Introduction

Complex supramolecular machineries in biological systems that perform crucial biological functions include DNA double helices, cell membranes, viral capsids, ribosomes, cytoskeleton and many others. Studying such model supramolecular systems from synthetic molecules in the laboratory has been quite rewarding as it provides better understanding of such phenomenon and possibly help to develop materials for various biomedical applications.[1-11] For example, self-assembly of small molecules leading to prion-like nanofibrils proved effective in killing cancer cells by impending cytoskeleton dynamics of cancer cells;[12] capsid protein of infectious cowpea chlorotic mosaic virus was reported to form vesicles without the viral genome.[13] The structure and functions of cell membranes were better understood from the contribution of Kunitake et al. who reported, for the first time, that a small organic molecule namely didodecyldimethylammonium bromide could form bilayer lamellar structure akin to cell membrane that subsequently resulted in multi-layered vesicles in polar solvent (water) upon sonication.[14] Since then, innumerous examples of vesicles derived from synthetic molecules have been reported.[15-20] Liu and Fujita[21,22] reported single layered vesicles having 'black berry' structure obtained through the self-assembly of cationic cage molecules such as metal organic polyhedra (MOP) in solution. Recently, we reported that single layered vesicle capable of loading and releasing an anti-cancer drug in a *p*H responsive fashion was obtained through the self-assembly of a Cu(II) based MOP nanocage molecule.[23] Research on organic cage molecules[24-29], on the other hand, gained an impetus in recent years due to their extraordinary permanent porosity with surface areas that rival even extended metal-organic frameworks.[30-32] However, literature survey indicates that vesicle derived from purely organic spherical molecule is hitherto unknown. It is easy to recognize the fact that vesicle obtained from spherical organic molecule is expected to be free from the plausible toxicity induced by metal ion (a major concern in biomedical applications) compared to its metal-organic counterpart (MOP). Studies revealed that both counterions and hydrophobic interactions played crucial roles in the self-assembly process of MOPs generating vesicles.[22] We, therefore, considered synthesizing cationic spherical organic molecules having large π-surface and studying their self-assembly properties leading to vesicles that might be useful in drug delivery applications (Scheme 1).

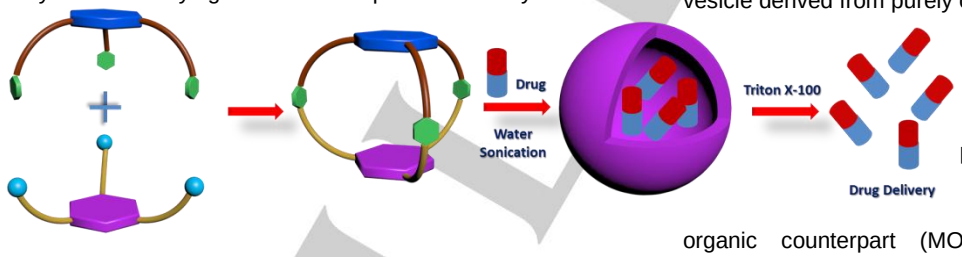

Scheme 1: Schematic overview of the work reported herein.

Results and Discussion

Synthesis and characterization

Straight forward synthesis starting from commercially available 1,3,5-triethyl benzene afforded **C_1-C_3** in good yield; ^{1}H and ^{13}C NMR supported the formation of **C_1-C_3** . The HRMS spectra showed prominent peaks which were attributed to *m/z* $[M\text{-}H^+]^{2+}$

[a] K. Sarkar, S. Ahmed and Prof. P. Dastidar
School of Chemical Sciences
Indian Association for the Cultivation of Science (IACS)
2A & 2B, Raja S. C. Mullick Road
Jadavpur, Kolkata, 700032, West Bengal (India)
Fax: (+91) 33-2473-2805
E-mail: ocpd@iacs.res.in
Supporting information for this article is given via a link at the end of the document.

376.0916 and $[M]^{3+}$ 251.0886 for **C_1**, $[M\text{-}H^+]^{2+}$ 355.1704 and $[M]^{3+}$ 237.1185 for **C_2** and $[M\text{-}CH_3^+]^{2+}$ 372.1395 and $[M]^{3+}$ 253.1035 for **C_3**; the experimental isotope distribution patterns also matched very well with that of the calculated patterns supporting the formation of **C_1-C_3** (Figure S4, supporting information).

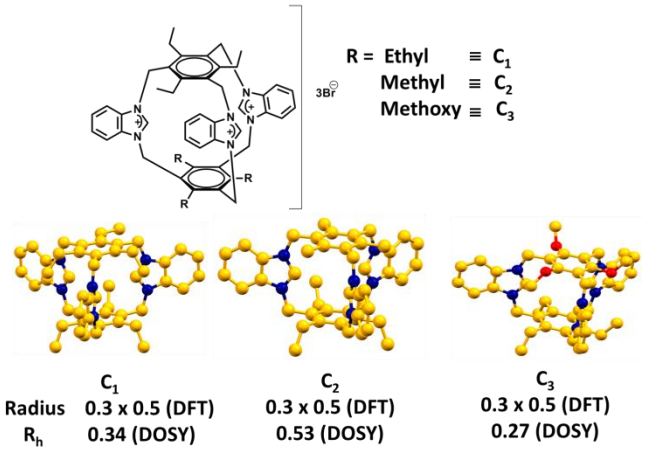

Scheme 2: Chemical and energy minimized structures (DFT) of **C_1-C_3**.

Further support came from DOSY NMR spectra in D_2O at room temperature. Peaks corresponding to all the protons of **C_1-C_3** were located on the same horizontal line in each case and therefore, had same diffusion coefficient ($D = 7.19\times10^{-10}$, 4.613×10^{-10} and 9.09×10^{-10} m^2/s for **C_1**, **C_2** and **C_3**, respectively) indicating the existence of discrete molecules in solution. The hydrodynamic radius (R_h = 0.34, 0.53 and 0.27 nm for **C_1**, **C_2** and **C_3**, respectively) obtained from the corresponding diffusion coefficients corroborated well with that of the single special molecule estimated from DFT energy minimized structures (Scheme 2) (Figure S5 and Table S1, supporting information).

Vesicle formation

The compounds were then tested for vesicle formation in water. In a typical procedure, measured amount of a compound (3 mg) was taken in milli-Q water (4 mL) in a vial and was sonicated for 15 min followed by vigorous shaking. Turbidity with frothing was observed in each case. It was then subjected to high resolution microscopy (TEM and AFM). Spherical objects with wide range of size (40-99, 44-195 and 39-287 nm for **C_1**, **C_2** and **C_3**, respectively) were observed in TEM images. Interestingly, similar spherical objects were also seen in AFM images and the height profile analyses indicated that they were most likely the flattened vesicles formed due to drying of the samples (Figure 1). These data strongly suggested vesicle formation due to the self-assembly of the spherical organic molecules in water. To provide further support, we then recorded DLS data of the compounds in water. Normal distribution of particle size within the range of 142–396, 190–295 and 396–825 nm for **C_1**, **C_2** and **C_3**, respectively observed in DLS were expectedly larger than the particle size observed in TEM as R_h of the particles in water were expected to be larger than that of the dried particles in TEM (Figure S7, supporting information). The data presented thus far clearly indicated that **C_1-C_3** could produce vesicles namely **vesicle(C_1), vesicle(C_2) and vesicle(C_3)** in water, respectively.

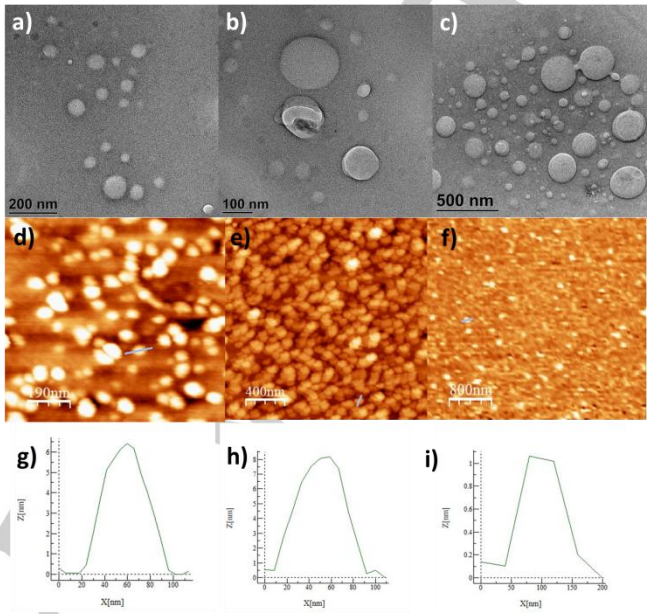

Figure 1: TEM [a)-c)] and AFM [d)-f)] images of dried samples of **C_1**, **C_2** and **C_3** in water, respectively; g)-i) the corresponding height profile of AFM images d)-f).

To evaluate whether the vesicles, thus obtained, were suitable as cargo to load and deliver drugs, we first loaded a hydrophilic dye namely calcein in the vesicles. In a typical experiment, both calcein and the spherical organic molecule were dissolved in milli-Q water by sonication and shaking. The extra-vesicular calcein was removed through dialysis following a standard protocol.[33] UV-vis spectra of **calcein@vesicle** were found to be red-shifted (13, 12 and 8 nm for **C_1**, **C_2** and **C_3**, respectively) compared to that of the free calcein indicating its confined environment. Significant quenching of the emission band (λ = ~510 nm) of calcein (compared to that of free calcein) in each case was observed when the **calcein@vesicle** were excited at λ = 450 nm suggesting that calcein molecules were indeed encapsulated within the vesicles.[34] Furthermore, calcein encapsulated vesicles were clearly observed through green fluorescence of **calcein@vesicle** under a fluorescence microscope (blue filter, λ = 480 nm).

Drug loading and its release

Following similar protocol, an anti-cancer drug namely doxorubicin hydrochloride (DOX) was loaded within the vesicles. The data revealed that **vesicle(C_3)** was found to be the most efficient in loading DOX (10.5 %) (Figure 2). Since all the vesicles reported herein were found to be stable up to pH 3 (Figure S8, supporting information), we explored a well-known vesicle destroyer[35] (Triton-X-100) in order to deliver the encapsulated drug in a stimuli responsive fashion. DLS data of all the vesicles in presence of Triton-X-100 (5 μL) showed

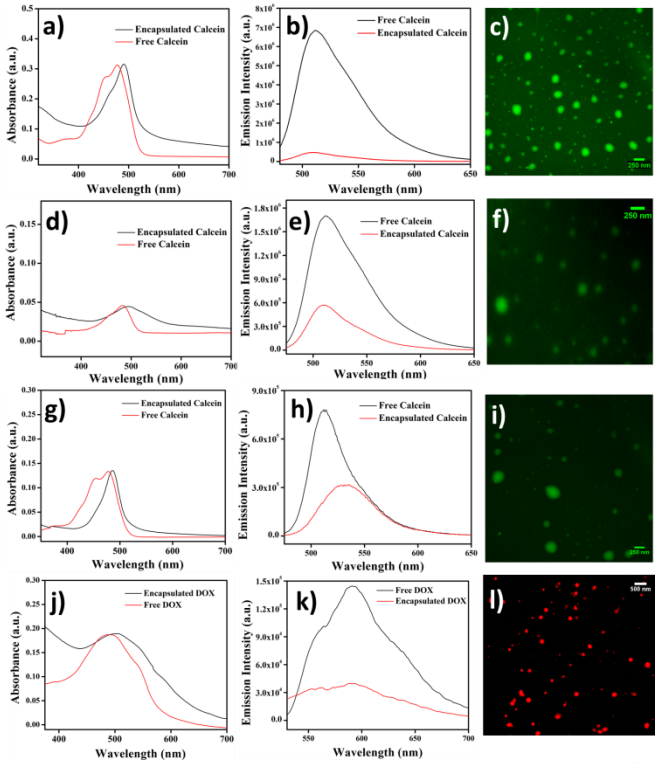

Figure 2: Comparative UV-vis spectra of the encapsulated calcein within a) **vesicle(C_1)**, d) **vesicle(C_2)**, g) **vesicle(C_3)** with free calcein; comparative photoluminescence spectra of encapsulated calcein within b) **vesicle(C_1)**, e) **vesicle(C_2)**, h) **vesicle(C_3)** with free calcein; fluorescence microscopic images of encapsulated calcein within c) **vesicle(C_1)**, f) **vesicle(C_2)**, i) **vesicle(C_3)**; j) comparative UV-vis and k) photoluminescence spectra of **DOX@vesicle(C_3)** with free DOX, l) the corresponding fluorescence microscopic image. Scale bars for c), f), i), l) are 250, 250, 250, 500 nm, respectively.

significantly smaller particle size (~10 nm) indicating disruption of the vesicular structures (Figure S9, supporting information). We decided to carry out further studies with **vesicle(C_3)** since its DOX loading capacity was the highest amongst all the vesicles studied herein. Photoluminescence studies revealed that Triton-X-100 was quite effective in releasing the encapsulated DOX from the vesicle (Figure S10, supporting information). The next task was to demonstrate that **DOX@vesicle(C_3)** could be utilized to deliver the drug in presence of Triton-X-100 *in vitro* on a cancer cell line.

However, it was important to evaluate the cytotoxicity of **C_3** on a normal cell before evaluating the possibility of delivery DOX from **DOX@vesicle(C_3)**. MTT assay[36] on mouse macrophage cell line (RAW 264.7) revealed that **C_3** was biocompatible up to 100 μM which was far superior to that of the Cu(II) MOP (0.6 μM) reported by us[23] (Figure S11, supporting information). To demonstrate that DOX could be released from **DOX@vesicle(C_3)** on cancer cells in presence of Triton-X-100, we carried out cell migration assay on a highly aggressive human breast cancer cell line MDA-MB-231. Cell migration is an essential activity in healthy cells. However, uncontrolled growth of cancer cells reflected through hyperactivity in cell migration leads to metastasis.[37,38]

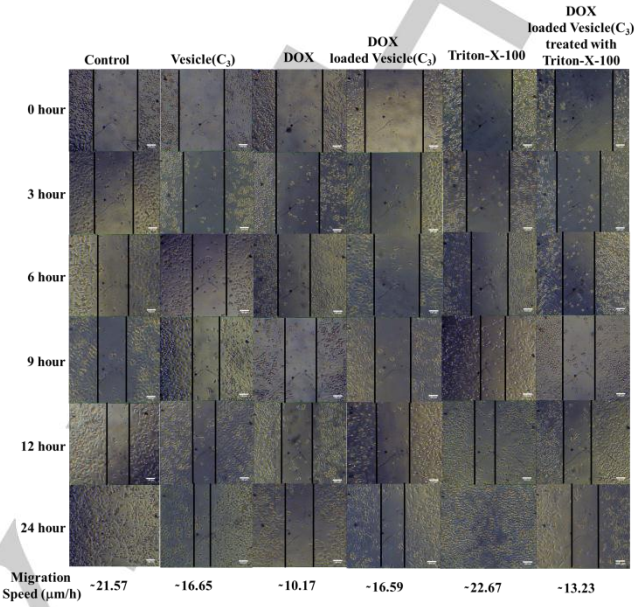

Figure 3: Cell migration assay. Scale bar = 100 μm.

Cell migration assay allows us to evaluate the anti-cancer property of a material *in vitro* by quantifying the speed with which the cancer cells migrate in presence of the material under study.[39,40] The slower the speed, the better is the anti-cancer property. After achieving confluency of the cells (MDA-MB-231) grown on a six well plate in an incubator, a gap was created on the plates by a scratch using a sterile microtip. Each well was then treated with the media (DMEM), **vesicle(C_3)**, DOX, **DOX@vesicle(C_3)**, Triton-X-100 and **DOX@vesicle(C_3)** containing Triton-X-100 – all in DMEM – keeping the concentration of the additives as listed in Table S2(supporting information). The progress of cell migration was monitored under an optical microscope for 24 h. The cells were completely merged in the cases of control (on DMEM) and Triton-X-100 suggesting no anti-cancer activity arising due to these materials. Whereas, in other cases, some amount of gap still remained after 24 h incubation. Nearly equal migration speed in presence of **vesicle(C_3)** and **DOX@vesicle(C_3)** (~16.6 μm/h) suggested that the anti-cancer drug DOX was tightly held within **vesicle(C_3)** and therefore, did not have a chance to retard the speed of migration of the cancer cells whereas, the cell migration speed in presence of DOX and **DOX@vesicle(C_3)** containing Triton-X-100 were found to be comparable (10.2 and 13.2 μm/h, respectively) indicating delivery of the confined drug in presence of vesicle destroyer Triton-X-100 (Figure 3).

To see whether **DOX@vesicle(C_3)** was also internalized, we carried out cell imaging studies with the same cell line.[41] Fluorescence image of the cells incubated in presence of **DOX@vesicle(C_3)** showed intense red color of DOX suggesting

successful internalization (Figure 4). Control experiment wherein the cells were incubated with DOX alone did not produce any color indicating that DOX itself could not penetrate the cell membrane (Figure S12). These data clearly established that **vesicle(C_3)** did act as a cargo to carry the payload (DOX) inside the cells (Figure 4).

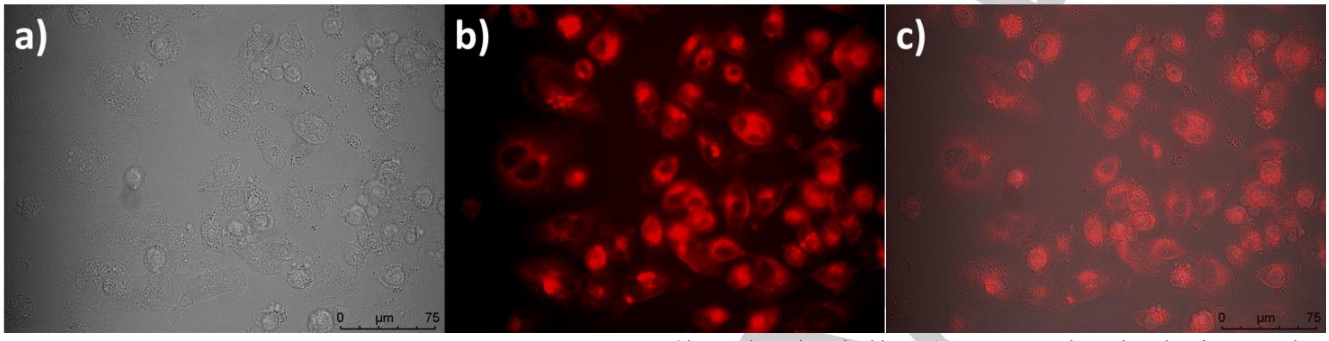

Figure 4: Fluorescence microscopic images of MDA-MB-231 cells incubated with **DOX@vesicle(C_3)**: a) bright field, b) fluorescence and c) overlay; Scale bar = 75 μm.

Conclusions

Thus, vesicle formation by the spherical organic molecules (**C_1-C_3**) is reported for the first time. **Vesicle(C_3)** could load an anti-cancer drug DOX and release it to a cancer cell in presence of a vesicle destroyer Triton-X-100 as revealed by cell migration assay with a highly aggressive human breast cancer cell line (MDA-MB-231). **DOX@vesicle(C_3)** was also successfully internalized as evident from cell imaging studies. The results presented herein open up avenue to develop vesicles derived from spherical organic molecules for drug delivery applications, which are understandably advantageous compared to that of its metal-organic counterpart such as MOPs because vesicles derived from purely organic molecules are free from metal-induced toxicity expected for MOP. The results presented herein indicate that vesicles may be developed from cationic organic cage molecules. Therefore, intriguing possibility of developing multi-drug delivery system by encapsulating two different drugs – one within the cage and the other within the vesicles is perhaps feasible. Attempts are being made to synthesize cationic orgnaic cage molecules following the same synthetic strategy adopted herein.

Experimental Section

Materials and Physical measurements:

All the chemicals were commercially available and used without further purification. FT-IR spectra were obtained on a FT-IR instrument (FTIR-8300, Shimadzu). Melting point (m.p.) was measured by electronic melting point apparatus. TEM images were recorded using a JEOL instrument with 300 mesh copper TEM grid. Diameter of the vesicle from TEM images was measured using ImageJ software (version- 1.41o/Java 1.8.0_45). AFM images were taken with an NTMDT instrument, model no. AP-0100 in semi contact-mode. UV−Vis spectroscopic measurements were carried out on a Hewlett-Packard 8453 diode array spectrophotometer equipped with a Peltier temperature controller. NMR spectra were recorded using 300, 400 and 500 MHz spectrometer (Bruker Ultrasheild Plus- 300, 400 and 500). Emission spectra were recorded with a Horiba Jobin Yvon Fluoromax-4 spectrofluorometer. Fluorescence images has been collected in light microscope (BX51, Olympus) equipped with a 100 W mercury lamp housing for an exciter and a excitation band filter covering wavelengths 420−440 nm. Dynamic light scattering experiments were executed using Malvern Particle Size Analyser (Model No. ZEN 3690 ZETASIZER NANO ZS 90 version 7.03). MTT assay were conducted using a multiplate ELISA reader (Varioskan Flash Elisa Reader, Thermo Fisher). Confocal microscopy was done in a C1 Nikon confocal microscopy.

Synthesis of C_1-C_3:

Step 1:
Synthesis of 1:
1,3,5-triethylbenzene (2 mL, 10.6 mmol), paraformaldehyde (3.38 g, 112.5 mmol), zinc bromide (3.94 g, 17.5 mmol) were taken in a round bottom (r.b) flask (250 mL) and HBr in glacial acetic acid (40 ml 33%) was then added. The mixture was then heated to 95 °C with constant stirring for 24 h. Precipitate was filtered, washed with water thoroughly and dried. 1,3,5-trimethyl-2,4,6-tribromomethylbenzene and 1,3,5-trimethoxy-2,4,6-tribromomethylbenzene were synthesized following similar procedure. 1,3,5-trimethylbenzene (1.47 mL, 10.6 mmol), paraformaldehyde (3.38 g, 112.5 mmol), zinc bromide (3.94 g, 17.5 mmol) were taken in a round bottom (r.b) flask (250 mL) and HBr in 50 glacial acetic acid (40 ml 33%) was added. The mixture was then heated to 95 °C with constant stirring for 24 h. Precipitate was filtered, washed with water thoroughly and dried. 1,3,5-trimethoxybenzene (1.78 g, 10.6 mmol), paraformaldehyde (3.38 g, 112.5 mmol) were taken in a round bottom (r.b) flask (250 mL) along with glacial acetic acid (20 mL) and stirred for 1 h. HBr in glacial acetic acid (40 ml 33%) was then added. The mixture was then heated to 65 °C with constant stirring for 24 h. Reaction mixture was then added to cold water taken in a beaker (500 mL) drop wise with constant stirring. Precipitate was filtered, washed with excess water and purified by column chromatography (4% ethyl acetate/petroleum ether).
Step 2:
Synthesis of 2:
Benzimidazole (2.67 g, 22.6 mmol) and KOH pellet (1.26 g, 22.6 mmol) were taken in a r.b flask (250 mL). Tetrahydrofuran (THF, 100 mL) was added into it and heated with stirring for 30 minutes. 1,3,5-triethyl-2,4,6-tribromomethylbenzene (2 g, 4.5 mmol) in THF (50 mL) was then added drop wise and refluxed overnight. The mixture was then evaporated in a rotary evaporator and the compound was extracted in dichloromethane and water solvent mixture. The organic layer was thoroughly washed with water and the compound was obtained by evaporating the dichloromethane in rotary evaporator.

Step 3:

Synthesis of the C_1:

A double necked round bottom flask (500 mL) was fitted with a reflux condenser and pressure equalizing funnel. A solution of Compound 2 (750 mg, 1.35 mmol) in a 1:2 Acetone-Chloroform mixtures (i.e. 80 mL Acetone + 160 mL $CHCl_3$) was added to the round bottom flask and stirred for 30 minutes at 50 - 60 ^oC. A solution of 1,3,5-triethyl-2,4,6-tribromomethylbenzene (595 mg, 1.35 mmol) in acetone (80 mL) was taken in the pressure equalizing funnel and added drop wise for a period of 2-3 h with vigorous stirring. A white precipitate started forming after 1.5 h. After the addition was complete, the pressure equalizing funnel was removed and closed the neck with a stopper. The mixture was stirred for another three days under reflux. Temperature was maintained to 90 ^oC. The white compound was obtained as a $3Br^-$ salt and was collected by evaporating the solvent in a rotary evaporator.

C_2 and **C_3** were synthesized following the same procedure by adding 1,3,5-trimethyl-2,4,6-tribromomethylbenzene (538 mg, 1.35 mmol) and 1,3,5-trimethoxy-2,4,6-tribromomethylbenzene (603 mg, 1.35 mmol) instead of 1,3,5-triethyl-2,4,6-tribromomethylbenzene, respectively.

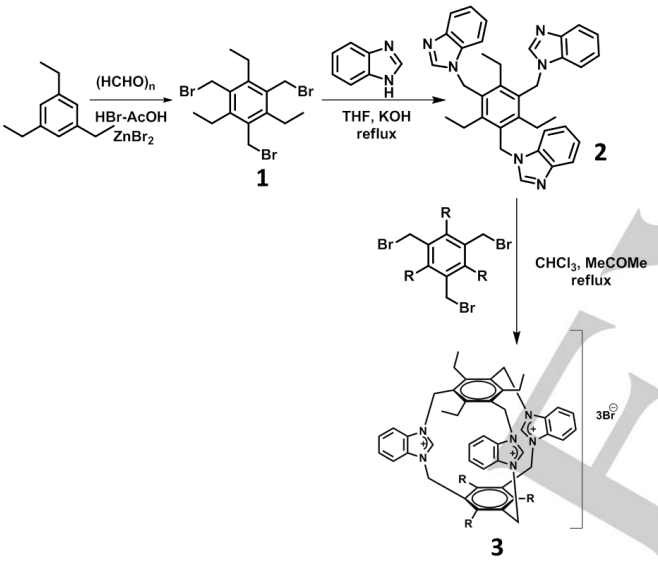

Scheme 3: Schematic representation of the reaction procedure.

Characterization data:

C_1: (White solid, m.p. > 250 °C, Yield: 79%); ^1H NMR (300 MHz, D_2O, 25°C): δ 8.26-8.23 (dd, 6H), 7.98-7.95 (dd, 6H), 6.42 (s, 3H), 5.82 (s, 12H), 2.54-2.47 (q, 12H), 1.26-1.21 (t, 18H) ppm; ^{13}C NMR (75 MHz, D_2O, 25°C): δ 149.16, 133.49, 132.96, 128.72, 128.67, 113.85, 45.38, 22.97, 15.20 ppm; HRMS (CH_3OH) *m/z*: Calculated for $[(C_{51}H_{57}N_6)^{3+}]$: 753.4628/3 = 251.1542; found: 251.0886; *m/z*: Calculated for $[(C_{51}H_{56}N_6)^{2+}]$: 752.4555/2 = 376.2277; found: 376.0916; FT-IR: 3404.08, 2970.2, 2931.4, 1615.6, 1572.95, 1483.64, 1453.29, 1322.08, 1230.61, 1183.62, 1133.8, 1001.3, 505.1 cm^{-1}.

C_2: (White solid, m.p. > 250 °C, Yield: 72%); ^1H NMR (300 MHz, D_2O, 25°C): δ 8.24-8.21 (dd, 6H), 7.98-7.95 (dd, 6H), 6.40 (s, 3H), 5.92 (s, 6H), 5.82 (s, 6H), 2.54-2.47 (q, 6H), 2.30 (s, 9H), 1.28-1.23 (t, 9H) ppm; ^{13}C NMR (126 MHz, D_2O, 25°C): δ 149.00, 142.59, 132.89, 132.74, 129.43, 128.55, 113.79, 113.72, 46.09, 45.02, 22.94, 15.16, 15.06 ppm; HRMS (CH_3OH) *m/z*: Calculated for $[(C_{48}H_{51}N_6)^{3+}]$: 711.4159/3 = 237.1386; found: 237.1185; *m/z*: Calculated for $[(C_{48}H_{50}N_6)^{2+}]$: 710.4086/2 = 355.2043; found: 355.1704; FT-IR: 3421.3, 3012.11, 2974, 1605.8, 1574.07, 1484.25, 1321.91, 1235.36, 1182.21, 1006.81, 761.33, 592.76, 507.84 cm^{-1}.

C_3: (White solid, m.p. > 250 °C, Yield: 64%); ^1H NMR (300 MHz, D_2O, 25°C): δ 8.18-8.10 (dd, 6H), 7.89-7.83 (dd, 6H), 5.75 (s, 9H), 5.68 (s, 3H), 3.94 (s, 6H), 3.79 (s, 6H), 2.47-2.40 (q, 6H), 1.18-1.12 (t, 9H) ppm; ^{13}C NMR (126 MHz, D_2O, 25°C): δ 148.82, 132.54, 128.63, 128.01, 118.95, 113.73, 113.47, 64.43, 63.69, 44.87, 41.84, 23.13, 15.07 ppm; HRMS (CH_3OH) *m/z*: Calculated for $[(C_{48}H_{51}N_6O_3)^{3+}]$: 759.4006/3 = 253.1335; found: 253.1035; *m/z*: Calculated for $[(C_{47}H_{48}N_6O_3)^{2+}]$: 744.3777/2 = 372.1888; found: 372.1395; FT-IR: 3390.75, 2980.9, 1595.1, 1562.84, 1452.48, 1325.99, 1186.11, 1101.62, 982.25, 747.58, 504.34 cm^{-1}.

DOSY NMR spectra :

Diffusion-Ordered Spectroscopy (DOSY) ^1H NMR was performed on a Bruker 400 and 500 MHz spectrometer with the magnetic field gradient (γ) 4.258×10^3 Hz/G .The length of the gradient (δ) for **C_1**, **C_2** and **C_3** was 1 ms, and the two pulsed gradients (Δ) for **C_1**, **C_2** and **C_3** was 200, 80 and 200 ms, respectively. All spectra were taken at room temperature. After the data collection, FIDs were processed and analyzed with the NMR software TopSpin 2.0 provided by Bruker.

Preparation of vesicles and characterization:

Compounds (3 mg) were taken in a separate vials and 4 mL milli-Q water was added [concentration of **C_1** = 754.7 μM, **C_2** = 788.1 μM, **C_3** = 750.2 μM]. The solutions were then sonicated for 15 minutes followed by vigorous shaking. Turbidity and bubbles appeared on the vials after sonication and shaking. The resulted dispersions were separately subjected for various analyses like DLS, TEM and AFM etc.

TEM sample preparation:

The water dispersion of the corresponding compounds were drop casted on a carbon-coated Cu (300 mesh) TEM grid. The grid was dried under vacuum at room temperature for one day and used for recording TEM images.

Atomic Force Microscopic (AFM) Study:

The water dispersions of the vesicles were drop-casted separately on mica and air dried for 24 h. It was then subjected for AFM analysis.

DLS analyses:

The dispersion of the vesicles were separately taken in a glass cuvette and subjected to the DLS experiment.

Calcein encapsulation within the vesicles:

Calcein (1.24 mg) was taken in a vial and methanol (1 mL) was added. The mixture was then heated and sonicated for several times to make a nearly homogeneous solution. An aliquot (100 μL) withdrawn from the solution and taken in another vial. The methanol was then evaporated to dryness by homogeneous gentle heating. The corresponding vesicles (3 mg) separately were added along with the addition of milli-Q water (4 mL). The mixture was then subjected to sonication followed by vigorous shaking. The resulting solution was then subjected to dialysis using SnakeSkin® dialysis tubing with molecular weight cut off 3500 for 72 hours following standard technique. Concentration of calcein inside the vesicles was estimated from UV-Vis spectra.

Sample preparation for fluorescence microscopy:

The aqueous solutions of the dye/drug encapsulated vesicles were separately drop-casted on a glass slide. The slide was then dried under ambient condition for one day and used for recording fluorescence images.

Doxorubicin encapsulation within the vesicle(C_3):

C_3 (4 mg) and solution of doxorubicin.HCl (DOX, 2 mL, 0.1 mg/mL) were taken in a vial and subjected to sonication followed by vigorous shaking. This mixture was then subjected to dialysis using SnakeSkin® dialysis tubing with molecular weight cut off 3500 for 72 hours following standard technique. Concentration of DOX inside **vesicle(C_3)** was estimated from UV-Vis spectra.

DOX release study:

The disruption of the vesicular assembly was studied in presence of two different stimuli, i.e. pH and in presence of Triton X-100.

For pH dependent disruption study, **vesicle(C_3)** (1 mL) was taken in a vial and the respective buffer solutions (1 mL) of different pH value (i.e. pH 7.4, 5.6 and 3.0) were added separately. The mixtures were then incubated for 1 h and subjected to DLS analysis. From the DLS data, it was quite clear that no disruption of the assembly of **vesicle(C_3)** was taking place with varying pH up to 3.0.

For Triton X-100 mediated disruption study, each of the vesicles (1 mL) separately were taken in a vial and Triton X-100 (5 μL) was added. The mixtures were then sonicated for 5 minutes and shaken vigorously. The mixtures were separately subjected to DLS analysis.

DOX release from the **vesicle(C_3)** has been established by treating DOX loaded **vesicle(C_3)** (1 mL) with Triton X-100 (5 μL) and sonicated followed by vigorous shaking. On the other hand, DOX loaded **vesicle(C_3)** solution (1 mL) was separately treated with buffer solution of pH 5.6 (1 mL) followed by sonication and vigorous shaking. These solutions were separately subjected to photoluminescence studies.

Biological studies

MTT assay:

RAW 264.7 macrophage cells and MDA-MB-231 cells were purchased from American Type Culture Collection (ATCC) and NCCS, Pune and maintained following their guidelines. The cells were cultured in Dulbecco's modified eagle's medium (DMEM) supplemented with 10% fetal bovine serum (FBS) and 1% penicillin–streptomycin and kept in a humidified incubator at 37° C and 5% CO_2.

The cytotoxicity of the **vesicle(C_3)** was evaluated in RAW 264.7 cells by using a standard MTT (3-(4,5-dimethylthiazol-2-yl)-2,5-diphenyltetrazolium bromide) assay. In a 96-well plates, the cells were seeded keeping density approximately 1×10^4 cells per well. After 24 h of seeding, the cells were treated with various concentrations of the **vesicle(C_3)** separately or DMEM alone for 72 h in a humidified incubator at 37° C and 5% CO_2. The culture medium was then replaced with 100 μg of MTT per well and kept at 37° C and 5% CO_2 for 4 h. The formazan produced by mitochondrial reductase from the live cells was dissolved by adding DMSO (100 μL per well) and incubated for 30 min at 37° C. The absorbance of the formazan was recorded at 570 nm by using a multiplate ELISA reader (Varioskan Flash Elisa Reader, Thermo Fisher). The percentages of survival of cells in presence of the respective **vesicle(C_3)** was calculated by considering the DMEM-treated sample to be 100%.

Cell migration studies:

MDA-MB-231 cells were seeded in a 6-well plate and kept in an incubator until the plates become almost confluent. A 200 μL sterile pipette tip was taken and scratched to generate a narrow path. The solutions were prepared by proper dilution with media to maintain an uniform concentration (Table S2). These solutions were added to the corresponding cells. For the control experiment, the cells were treated with only media. Still images were taken under an optical microscope (OLYMPUS CKX31, 10x) after different time intervals for 24 h to measure the migration speed.

Cell imaging:

For cell imaging, MDA-MB-231 cells were cultured by using DMEM supplemented with 10% FBS and 1% penicillin–streptomycin on ethanol etched cover slips kept in a 35 mm tissue culture dishes. The dishes were then kept in a humidified incubator at 37° C overnight. The cells were then washed with PBS and incubated in serum-free media (SFM) for half an hour. DOX encapsulated **vesicle(C_3)** was then taken in SFM keeping the concentration of **vesicle(C_3)** at IC_{50} concentration and DOX = 0.9 μM and added to the cells. It was then incubated for 30 min. After incubation, SFM was discarded followed by washing with PBS. The cells were fixed by using 4% paraformaldehyde for 10 min at room temperature. After fixing, the cells were washed with PBS and mounted on glass slides for microscopy. For control experiment, only DOX solution was taken in SFM keeping the concentration of DOX = 0.9 μM.

Acknowledgements

K.S thanks CSIR, IACS and S.A thanks CSIR for research fellowship. P.D thanks DST (EMR/2016/000894) for financial support. We thank Mr. Shanti Gopal Patra, School of Chemical Sciences, IACS for helping in DFT calculations.

Keywords: Spherical organic compounds • Vesicle • Drug delivery • Cell migration • Supramolecular chemistry

[1] K. Ariga, D. T. Leong, T. Mori, *Adv. Funct. Mater.* **2018**, *28*, 1702905.
[2] B. Schwarz, M. Uchida, T. Douglas, *Advances in virus research* **2017**, *97*, 1-60.
[3] J. Boucard, C. Linot, T. Blondy, S. Nedellec, P. Hulin, C. Blanquart, L. Lartigue, E. Ishow, *Small* **2018**, *14*, 1802307.
[4] S. Jia, W.-K. Fong, B. Graham, B. J. Boyd, *Chem. Mater.* **2018**, *30*, 2873−2887.
[5] O. J. G. M. Goor, S. I. S. Hendrikse, P. Y. W. Dankers, E. W. Meijer, *Chem. Soc. Rev.* **2017**, *46*, 6621—6637.
[6] N. Singh, M. Kumar, J. F. Miravet, R. V. Ulijn, B. Escuder, *Chem. Eur. J.* **2017**, *23*, 981 – 993.
[7] C. G. Palivan, R. Goers, A. Najer, X. Zhang, A. Car, W. Meier, *Chem. Soc. Rev.* **2016**, *45*, 377—411.
[8] X. Du, J. Zhou, J. Shi, B. Xu, *Chem. Rev.* **2015**, *115*, 13165−13307.
[9] M. J. Webber, R. Langer, *Chem. Soc. Rev.* **2017**, *46*, 6600-6620.
[10] S. S. Babu, V. K. Praveen, A. Ajayaghosh, *Chem. Rev.* **2014**, *114*, 1973-2129.
[11] E. Arunkumar, P. Chithra, A. Ajayaghosh, *J. Am. Chem. Soc.* **2004**, *126*, 6590-6598.
[12] Y. Kuang, M. J. C. Long, J. Zhou, J. Shi, Y. Gao, C. Xu, L. Hedstrom, B. Xu, *J. Biol. Chem.* **2014**, *289*, 29208-29218.
[13] L. Lavelle, M. Gingery, M. Phillips, W. M. Gelbart, C. M. Knobler, *J. Phys. Chem. B* **2009,** *113,* 3813–3819.
[14] T. Kunitake, Y. Okahata, *J. Am. Chem. Soc.* **1977**, *99*, 3860-3861.
[15] N. Sakai, S. Matile, *Nat. Chem.* **2009**, *1*, 599-600.
[16] R. Dong, Y. Zhou, X. Zhu, *Acc. Chem. Res.* **2014**, *47*, 2006−2016.
[17] J. Voskuhl, B. J. Ravoo, *Chem. Soc. Rev.* **2009**, *38*, 495–505.
[18] T. Kunitake, *Angew. Chem. Int. Ed. Engl.* **1992**, *31*, 709-726.
[19] L. E. Euliss, J. A. DuPont, S. Gratton, J. DeSimone, *Chem. Soc. Rev.* **2006**, *35*, 1095–1104.
[20] E. Fleige, M. A. Quadir, R. Haag, *Adv. Drug Deliv. Rev.* **2012**, *64*, 866–884.
[21] D. Li, J. Zhang, K. Landskron, T. Liu, *J. Am. Chem. Soc.* **2008**, *130*, 4226-4227.

[22] D. Li, W. Zhou, K. Landskron, S. Sato, C. J. Kiely, M. Fujita, T. Liu, *Angew. Chem.* **2011**, *123*, 5288 –5293.
[23] K. Sarkar, M. Paul, P. Dastidar, *Chem. Commun.* **2016**, *52*, 13124—13127.
[24] T. Hasell, A. I. Cooper, *Nat. Rev. Mater.* **2016**, *1*, 16053.
[25] X. Kong, J. Jiang, *J. Phys. Chem. C* **2018**, *122*, 1732−1740.
[26] K. Acharyya, P. S. Mukherjee, *Chem. Eur. J.* **2015**, *21*, 6823 – 6831.
[27] G. Zhang, O. Presly, F. White, I. M. Oppel, M. Mastalerz, *Angew. Chem. Int. Ed.* **2014**, *53*, 1516 –1520.
[28] V. Amendola, M. Boiocchi, L. Fabbrizzi, N. Fusco, *Eur. J. Org. Chem.* **2011**, 6434–6444.
[29] V. Amendola, G. Bergamaschi, M. Boiocchi, L. Fabbrizzi, N. Fusco, *Dalton Trans.* **2011**, *40*, 8367–8376.
[30] C. A. Trickett, A. Helal, B. A. Al-Maythalony, Z. H. Yamani, K. E. Cordova, O. M. Yaghi, *Nat. Rev. Mater.* **2017**, *2*, 17045.
[31] M. Woellner, S. Hausdorf, N. Klein, P. Mueller, M. W. Smith, S. Kaskel, *Adv. Mater.* **2018**, *30*, 1704679.
[32] K. Adil, Y. Belmabkhout, R. S. Pillai, A. Cadiau, P. M. Bhatt, A. H. Assen, G. Maurin, M. Eddaoudi, *Chem. Soc. Rev.* **2017**, *46*, 3402—3430.
[33] K. Dan, S. Ghosh, *Angew. Chem.* **2013**, *125*, 7441 –7446.
[34] A. Sikder, A. Das, S. Ghosh, *Angew. Chem. Int. Ed.* **2015**, *54*, 6755 –6760.
[35] C. Hu, N. Ma, F. Li, Y. Fang, Y. Liu, L. Zhao, S. Qiao, X. Li, X. Jiang, T. Li, F. Shen, Y. Huang, Q. Luo, J. Liu, *ACS Appl. Mater. Interfaces* **2018**, *10*, 4603−4613.
[36] Q.-S. Wang, Y. Xiang, Y.-L. Cui, K.-M. Lin, X.-F. Zhang, *PLoS One* **2012**, *7*, e34122.
[37] J. J. Bravo-Cordero, L. Hodgson, J. Condeelis, *Curr. Opin. Cell Biol.* **2012**, *24*, 277−283.
[38] D. Hanahan, R. A. Weinberg, *Cell* **2011**, *144*, 646−674.
[39] C.-C. Liang, A. Y. Park, J.-L. Guan, *Nat. Protoc.* **2007**, *2*, 329-333.
[40] J. Deb, J. Majumder, S. Bhattacharyya, S. S. Jana, *BMC Cancer* **2014**, *14*, 567.
[41] Y. Zhang, N. Kohler, M. Zhang, *Biomaterials* **2002**, *23*, 1553–1561.

10.1002/asia.201900211

Entry for the Table of Contents

FULL PAPER

Vesicle derived from cationic spherical organic molecules showed stimuli responsive release of the drug.

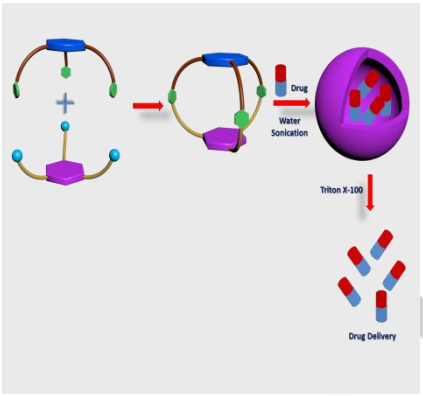

*Koushik Sarkar, Sabir Ahmed and Parthasarathi Dastidar**

Page No. – Page No.

Self-assembly of Spherical Organic Molecules to form Hollow Vesicular Structure in Water for Encapsulation of an Anti-cancer Drug and Its Release